Lipid Raft Composition Modulates Sphingomyelinase Activity and Ceramide-Induced Membrane Physical Alterations

Liana C. Silva,[†‡*] Anthony H. Futerman,[‡] and Manuel Prieto[†]
[†]Centro de Química-Física Molecular & Institute of Nanoscience and Nanotechnology, Instituto Superior Técnico, Lisbon, Portugal; and [‡]Department of Biological Chemistry, Weizmann Institute of Science, Rehovot, Israel

ABSTRACT Lipid rafts and ceramide (Cer)-platforms are membrane domains that play an important role in several biological processes. Cer-platforms are commonly formed in the plasma membrane by the action of sphingomyelinase (SMase) upon hydrolysis of sphingomyelin (SM) within lipid rafts. The interplay among SMase activity, initial membrane properties (i.e., phase behavior and lipid lateral organization) and lipid composition, and the amount of product (Cer) generated, and how it modulates membrane properties were studied using fluorescence methodologies in model membranes. The activity of SMase was evaluated by following the hydrolysis of radioactive SM. It was observed that 1), the enzyme activity and extent of hydrolysis are strongly dependent on membrane physical properties but not on substrate content, and are higher in raft-like mixtures, i.e., mixtures with liquid-disordered/liquid-ordered phase separation; and 2), Cer-induced alterations are also dependent on membrane composition, specifically the cholesterol (Chol) content. In the lowest-Chol range, Cer segregates together with SM into small (~8.5 nm) Cer/SM-gel domains. With increasing Chol, the ability of Cer to recruit SM and form gel domains strongly decreases. In the high-Chol range, a Chol-enriched/SM-depleted liquid-ordered phase predominates. Together, these data suggest that in biological membranes, Chol in particular and raft domains in general play an important role in modulating SMase activity and regulating membrane physical properties by restraining Cer-induced alterations.

INTRODUCTION

Evidence points to the existence of distinct lateral domains in cell membranes that have unique physical properties different from those of the bulk membrane, and are thought to be responsible for the modulation of several biological processes. Among membrane domains, the most common are lipid rafts, which are regarded as ordered regions (liquid-ordered phase, l_o) enriched in cholesterol (Chol) and sphingolipid (SL), and float in the fluid membrane (liquid-disordered phase, l_d) (1). Lipid rafts were shown to be involved in cell signaling, lipid and protein sorting, and membrane trafficking (2,3). Recently, ceramide (Cer)-platforms also emerged as an important class of membrane domains with numerous biological roles, including apoptotic signaling cascades and viral and bacterial entry (4,5). Similarly to lipid rafts, the specific physical characteristics of Cer-platforms are thought to be responsible for the biological effects of these domains (6). In response to a stress signal, Cer is generated in the plasma membrane through activation of the enzyme sphingomyelinase (SMase). SMase hydrolyzes sphingomyelin (SM), which is involved in lipid raft formation. Therefore, these platforms are also believed to drive strong membrane reorganization.

Several studies carried out in model membranes addressed the effects of Cer on membrane biophysical properties upon preincorporation into the vesicles (7–10) or generation by SMase (11,12). In the first case, alterations induced by Cer in phase characteristics and domain topology and morphology were extensively studied in different lipid mixtures (13). It is known that Cer segregates into highly ordered gel domains, increases the order of the fluid lipids, and facilitates the transition to nonlamellar phases (14,15). Literature regarding the alterations induced by the generation of Cer is scarcer (16–19), but evidence points to the formation of Cer-enriched domains and reorganization of the remaining lipids in the membrane. However, the nature and characteristics of the domains, and whether they are formed by Cer itself or together with other lipids are still subjects of debate.

Regarding SMase, several reports have addressed the kinetic characterization and the factors that modulate/regulate the activity of this interfacial enzyme, such as lateral packing and thermotropic phase transitions. It is recognized that membrane physical characteristics affect SMase activity (20), including fluidity (12,21), initial membrane composition and topography (22), surface pressure (23), and molecules, including lipids, that perturb the membrane (24).

It is also known that Cer-induced alterations on membrane biophysical properties are dependent on the initial lipid composition (8,9), specifically the Chol content. However, in the absence of detailed analysis, it is difficult to establish the relationship among the enzyme activity (i.e., the ability to hydrolyze the substrate), the initial membrane composition, and the resultant physical characteristics, and how the amount of product formed modulates the properties of the different membranes.

In this study we investigated the effect of substrate concentration/membrane physical properties on SMase activity by taking advantage of the well-characterized gel-fluid 1-palmitoyl-2-oleoyl-*sn*-glycero-3-phosphocholine (POPC)/*N*-palmitoyl-sphingomyelin (PSM) binary (25) and

Submitted August 1, 2008, and accepted for publication December 11, 2008.

*Correspondence: lianacsilva@ist.utl.pt

Editor: Thomas J. McIntosh.

0006-3495/09/04/3210/13 $2.00

doi: 10.1016/j.bpj.2008.12.3923

l_d-l_o POPC/PSM/Chol ternary (25,26) systems. Additionally, the membrane-induced physical alterations and lipid reorganization induced by the generated *N*-palmitoyl-Cer (PCer) were also extensively characterized. The results show that 1), enzyme activity is strongly dependent on membrane properties but not on substrate concentration, being higher in raft-like mixtures, i.e., mixtures presenting l_d-l_o phase separation; and 2), PCer-induced alterations are also dependent on the initial membrane composition, specifically the Chol content. In the lowest-Chol range, PCer segregates together with PSM into small (~8.5 nm) PCer/PSM gel domains. With increasing Chol, the ability of PCer to recruit PSM decreases, and the amount of gel phase is lower and becomes only PCer-enriched. In the high-Chol range, a Chol-enriched/PSM-depleted l_o phase predominates.

MATERIALS AND METHODS

Materials

POPC, PCer, PSM, and Rho-DOPE (1,2-dioleoyl-*sn*-glycero-3-phosphoethanolamine-*N*-(lissamine rhodamine B sulfonyl)) were obtained from Avanti Polar Lipids (Alabaster, AL). NBD-DPPE (1,2-dipalmitoyl-*sn*-glycero-3-phosphoethanolamine-*N*-(7-nitro-2-1,3-benzoxa-diazol-4-yl)) and t-PnA (*trans*-parinaric acid) were obtained from Molecular Probes (Leiden, The Netherlands). Chol and SMase isolated from *Bacillus cereus* were obtained from Sigma (St. Louis, MO). [^{3}H]-PSM was obtained from American Radiolabel (St. Louis, MO). All organic solvents were Uvasol grade from Merck.

Liposome preparation

Binary POPC/PSM and three-component multilamellar vesicles (MLVs) containing 72:23:5 (T2), 60:26:14 (T3), 45:30:25 (T4), 34:33:33 (T5), 25:35:40 (T6), and 15:37:48 (T7) POPC/PSM/Chol (Fig. 1) were prepared as previously described (9), with minor modifications. (To simplify the text, binary mixtures are denoted as BX_{PSM}, where X_{PSM} refers to the fraction of PSM present in the mixture, and ternary mixtures are denoted as T1–T7. T2–T6 ternary mixtures are contained within a tie-line that spans the 1:1:1 composition in the POPC/PSM/Chol ternary phase diagram, whereas T1 and T7 lie in the ld and lo phase, respectively (25) (see Fig. 1 *A*). T1 has the same composition as B20. The binary and ternary mixtures used in the study are represented in Fig. 1.) Briefly, lipid and probe stock solutions in chloroform (except for t-PnA; see below), were mixed at the desired molar ratios and dried until the solvent was completely evaporated (first under a stream of N2 and then under vacuum). To optimize the conditions for SMase activity (21), the lipid film was hydrated with Hepes 10 mM, NaCl 200 mM, CaCl2 10 mM, MgCl2 2 mM buffer, pH 7.4 (note that changing the suspension medium in comparison to previous studies (9,15,25) had no effect on the photophysical parameters of the probes; data not shown). The lipid suspension was repeatedly vortexed, followed by freeze-thaw cycles (up to eight times) using liquid nitrogen and a bath warmed to 50°C. For studies with t-PnA, samples were slowly brought to room temperature and the probe was then added from an ethanol stock solution (the final ethanol volume was always less than 0.5%, to prevent bilayer destabilization (27)). The samples were again reequilibrated by freeze-thaw cycles and subsequently kept overnight at 4°C. Before measurements were obtained, the samples were slowly brought to room temperature (24°C) and maintained at that temperature at least for 1 h.

Large unilamellar vesicles (LUVs) were obtained from MLVs by means of the extrusion technique. The extrusion procedure was carried out at 50°C to ensure that all lipids were in the fluid phase. The liposomes were subsequently kept overnight at 4°C. Before the measurements were initiated, the samples were slowly heated to the required temperature (24°C) and incubated for at least 1 h. The probe/lipid (P/L) ratios used were 1:200 for NBD-DPPE, 1:100 for Rho-DOPE, and 1:500 for t-PnA.

The concentration of POPC, PSM, Chol, and PCer stock solutions was determined gravimetrically with a high precision balance (UMT2; Mettler Toledo, Columbus, OH). Probe concentrations were determined spectrophotometrically using ε(t-PnA, 299.4 nm, ethanol) = 89×10^3 $M^{-1}cm^{-1}$ (28); ε(NBD-DPPE, 458 nm, chloroform) = 21×10^3 $M^{-1}cm^{-1}$; and ε(Rho-DOPE, 559 nm, chloroform) = 95×10^3 $M^{-1}cm^{-1}$ (29).

Absorption and fluorescence

All measurements were performed in 0.5 cm × 0.5 cm quartz cuvettes under magnetic stirring. The absorption and steady-state fluorescence instrumentation was as previously described (30). The absorption spectra were corrected for turbidity. Steady-state fluorescence measurements were performed using previously described (9) excitation (λ_{exc})/emission (λ_{em}) wavelengths (358/430 nm for DPH, 465/536nm for NBD-DPPE, and 570/593 nm for Rho-DOPE), except for t-PnA, for which 320 nm/405 nm was used. This wavelength was chosen to prevent excitation of the Trp residues of SMase. To check that the data were not affected by λ_{exc}, control experiments were carried out in POPC/PSM/Chol and POPC/PCer mixtures under previously described conditions (9,15). The results were essentially the same (data not shown). All measurements were performed at 24°C using a Julabo F25 circulating water bath (Houston, TX) to maintain constant temperature and controlled with 0.1°C precision directly inside the cuvette with a thermocouple.

Time-resolved fluorescence measurements with t-PnA were performed using λ_{exc} = 320 nm (secondary laser of 4-dicyanomethylene-2-methyl-6-(p-dimethylaminostyril)-4H-pyrane (DCM) (25)) and λ_{em} = 405 nm. For NBD-DPPE, λ_{exc} = 428 nm (Ti-Sapphire laser (26)) and λ_{em} = 536 nm were used. The data were analyzed as previously described (30). For a decay

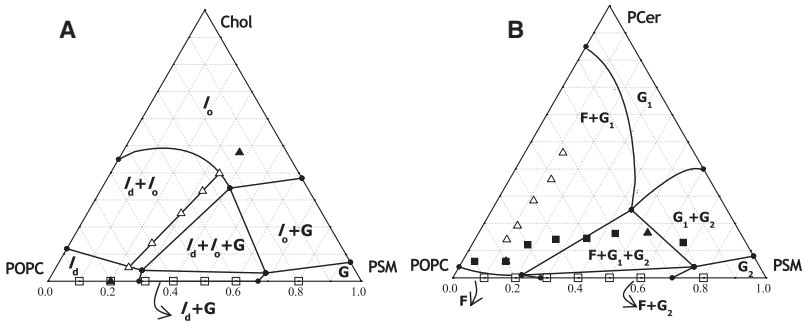

FIGURE 1 Ternary phase diagrams of (*A*) POPC/PSM/Chol (25) and (*B*) POPC/PSM/PCer (8). The ternary mixtures used in this study are represented in *A*. The solid triangles correspond to T1 and T7, the mixtures that are located in the one-phase region of the diagram (l_d and l_o, respectively), whereas the open triangles are the raft mixtures (T2–T6). l_d, l_o, and G are the liquid-disordered, liquid-ordered, and gel phases, respectively. See De Almeida et al. (25) for further details. The binary mixtures used in this study are represented in both *A* and *B* as open squares. The solid squares in *B* represent the mixtures that result from 2 h hydrolysis of the binary POPC/PSM vesicles. In *B* (△,▲) correspond to the hydrolysis of the raft and nonraft ternary POPC/PSM/Chol mixtures, respectively. For these mixtures, the ratio between POPC, PSM-remaining, and PCer-formed was calculated assuming that Chol was not interfering with PCer/PSM interaction. F, G_1, and G_2 are the fluid, Cer-rich, and PSM-rich gel phases, respectively. See Castro et al. (8) for further details.

described by a sum of exponentials, where α_i is the normalized preexponential and τ_i is the lifetime of the decay component i, the lifetime-weighted quantum yield and the mean fluorescence lifetime are given by: $\overline{\tau} = \sum_i \alpha_i \tau_i$ and $\langle \tau \rangle = \sum_i \alpha_i \tau_i^2 / \sum_i \alpha_i \tau_i$, respectively.

Characterization of SMase activity and PCer quantification

To follow PSM hydrolysis and PCer generation, the fluorescence anisotropy of the probes was measured as a function of time, at room temperature. The reaction was initiated 150 s after starting the measurements by direct addition of SMase (final enzyme concentration of 1 U/mL) to a magnetically stirred quartz cuvette containing LUVs (0.3 mM total lipid concentration) with the above-mentioned composition. Fluorescence anisotropy was measured each 5 s and up to 2 h after starting the reaction. Typically, a plateau in the anisotropy values was reached at $t < 10$ min.

To quantify the amount of PCer generated, lipid vesicles containing ~60 nCi of [^{3}H]-PSM per aliquot were prepared as described above. The reaction was started by adding 1 U/mL of SMase to each mixture. Aliquots were taken at defined times and the reaction was stopped by adding $CHCl_3$/methanol (1:2 v/v). The samples were loaded onto a thin-layer chromatography silica plate, and [^{3}H]-PSM and [^{3}H]-PCer were separated using $CHCl_3$/methanol/9.8 mM $CaCl_2$ (60:35:8 v/v/v) as the developing solvents. Lipids were visualized by using a phosphorimaging screen (Fuji, Tokyo, Japan) and recovered from the TLC plates by scraping the silica into scintillation vials. Then 1 mL of methanol and 5 mL of Optima Gold Scintillation fluid (Packard, Downers Groove, IL) were added to each vial and radioactivity was quantified using a Packard 2100 β radiospectrometer.

Förster resonance energy transfer experiments

Förster resonance energy transfer (FRET) experiments were carried out in LUVs (1 mM total lipid concentration) containing 1), NBD-DPPE/Rho-DOPE as the donor/acceptor (D/A) pair for FRET between l_o and l_d phases; or 2), t-PnA/NBD-DPPE for FRET between the gel and l_o phases. The P/L ratios were 1/1000 and 1/100 for donors and acceptors, respectively. For this donor P/L ratio, no donor self-quenching or energy homotransfer takes place (31). To determine the effect of enzyme action on FRET efficiency, and therefore on lipid reorganization, fluorescence lifetimes of the probes were measured in the absence of SMase and 2 h after addition of SMase to the mixtures.

Data analysis was carried out as described by De Almeida et al. (26) (see also Eqs. S3–10 in the Supporting Material for details of the model). The FRET efficiency, E, was obtained from the time-resolved fluorescence intensity curves, through the relation $E = 1 - \overline{\tau}_{DA}/\overline{\tau}_D$. (See also Silva et al. (9) for a detailed discussion regarding FRET variation for these D/A pairs in ternary mixtures in the absence of SMase.)

RESULTS

Rationale for selecting the lipid mixtures and experimental design

To study the interplay between membrane lipid composition and phase properties, and its effects on both SMase activity and Cer-induced alterations in membrane properties, two types of mixtures—POPC/PSM binary and POPC/PSM/Chol ternary—were selected because 1), their phase behavior is well established; and 2), the photophysical properties of the selected probes in these mixtures were previously studied in detail (9,25,26). For the specific case of ternary mixtures, their composition was selected so that they would be contained within a tie-line that spans the l_d-l_o phase coexistence region of the POPC/PSM/Chol ternary phase diagram (25). Among the several possible tie-lines, the one that spans the mixture presenting the 1:1:1 composition was chosen (Fig. 1 *A*), not only because this is considered the canonical raft mixture (32), but also because the mixtures that define this tie-line have been extensively studied in terms of both phase properties and domain size (26). It was essential to perform the study along a tie-line because in this case the composition of each phase is constant (given by the extremes of the tie-line) and only the fraction of the phases changes between the mixtures (lever rule), allowing for a direct comparison of the results obtained with the different mixtures (26,33). To simplify the text, the ternary mixtures that present l_d-l_o phase separation (T2–T6), and therefore mimic rafts, will also be referred to as raft mixtures.

The use of two types of mixtures makes it possible to perform studies under strict control of the system parameters, i.e., by using 1), mixtures with the same substrate content and different phase properties (e.g., l_d phase and l_o/l_d phase coexistence, gel/fluid and l_o/l_d phase coexistence, and gel/fluid phase coexistence and l_o phase, in binary and ternary mixtures, respectively); 2), mixtures with similar phase properties and different lipid compositions, in terms of only the substrate content or other lipid components as well (e.g., binary and ternary mixtures forming the same phase (l_d phase)); and 3), mixtures in which all the relevant phases formed by SM vary, such as l_d, gel/fluid, and gel in binary mixtures, and l_d, l_d/l_o, and l_o in ternary mixtures (see Fig. 1, where the mixtures under study are plotted and the respective phase properties are identified).

To obtain detailed information concerning membrane composition and the SMase/Cer interplay, two sets of experiments were designed. First, to relate enzyme activity with membrane properties/lipid composition, the activity of SMase was thoroughly studied in each of the mixtures. In this way, information regarding whether SMase activity is controlled by the phase properties or by the substrate concentration could be obtained. Second, the amount of PCer formed in each condition was determined and the alterations induced by this lipid on the membrane physical properties were then studied using fluorescence spectroscopy. This type of experiment provides information about the ability of PCer to change the membrane properties, and the relation between the amount of PCer that is required to, e.g., induce the formation of PCer-domains and how this lipid is able to interact with the other lipid components of the membrane. This set of experiments was also used to verify whether PCer generated from SMase is able to induce the formation of large domains (Cer-platforms), and to define the nature of those domains.

Characterization of SMase activity

Fig. 2 shows the percentage of substrate hydrolyzed versus time for binary POPC/PSM and ternary POPC/PSM/Chol mixtures (Fig. 2, *A* and *B*, respectively). Under the conditions

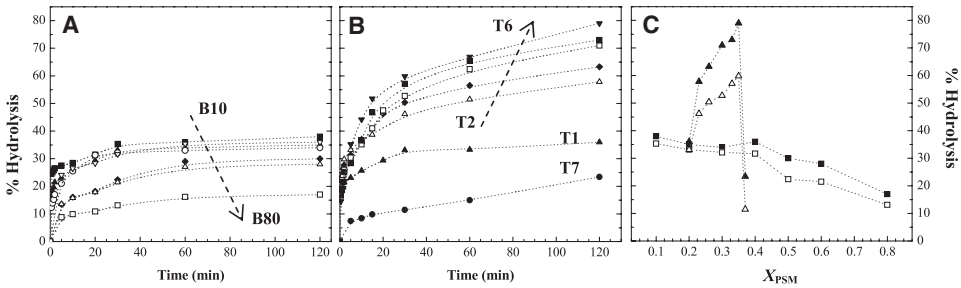

FIGURE 2 Relation among SMase activity, substrate content, and membrane properties. (*A* and *B*) Percentage of substrate hydrolyzed versus time in (*A*) POPC/PSM binary mixtures containing (■) 10, (▲) 20, (○) 30, (▽) 40, (◆) 50, (△) 60, and (□) 80% PSM, respectively; and (*B*) POPC/PSM/Chol ternary mixtures containing (▲) 20 (T1), (△) 23 (T2), (◆) 26 (T3), (□) 30 (T4), (■) 33 (T5), (▼) 35 (T6), and (•) 37% (T7) PSM, respectively. (*C*) Percentage of substrate hydrolyzed 30 min (*open symbols*) and 2 h (*solid symbols*) after starting the SMase reaction in binary (□, ■) and ternary (△, ▲) mixtures. The values are the means of at least three independent experiments. The standard deviation (SD) was always <3%.

used in the experiment, SMase readily hydrolyzes PSM with all of the lipid compositions studied. The reaction proceeds until a plateau is reached. However, the percentage of hydrolysis is not directly related to the amount of substrate in the reaction mixture. Thus, for binary mixtures, the percentage of hydrolysis decreases with PSM content (Fig. 2, *A* and *C*) and is always lower in comparison with the ternary mixtures containing the same amount of substrate (Fig. 2, *B* and *C*). Of interest, in the ternary mixtures, PSM hydrolysis increases while going along the tie-line that spans the raft region in the 1:1:1 mixture (T2–T6) (Fig. 1 *A*). However, for the two ternary mixtures that lie outside the coexistence region in the l_d and l_o phases (T1 and T7, respectively), the extent of hydrolysis is much lower. Note that increasing PSM by as little as 2% in this 100% l_o ternary mixture (T7) leads to a sharp decrease in the amount of hydrolysis (Fig. 2, *B* and *C*). This suggests that enzyme activity is dependent on the phase composition of the mixtures, and sharply increases in the raft region (T2–T6). When only the l_d or l_o phase is present, the hydrolysis efficiency is much lower, suggesting that the presence of domain interfaces in the membrane, formed as a consequence of phase separation, facilitate access of the enzyme to the substrate, as previously described for other interfacial enzymes (34) and suggested for SMase (17,19,20). However, there is less hydrolysis in mixtures that present gel-fluid phase coexistence, and thus packing defects, than in mixtures where only the fluid phase (l_d) is present, which shows that although these defects may facilitate SMase action, this is not the only parameter that governs enzyme activity.

It should be stressed that for the ternary raft mixtures, the amount of substrate hydrolyzed is higher than 50%, as previously observed for other SM-containing bilayers (16), which suggests that lipid translocation across the two leaflets takes place. Indeed, it was reported that Cer generation in the membrane increases the ability of the other membrane lipids to translocate (11).

To further explore how SMase activity is regulated by the product of reaction, the amount of PCer formed (Fig. 3 *A*) was determined. The fraction of PCer formed, X_{PCer}, increases for the ternary mixtures along the tie-line and is lower for the other mixtures. In addition, a plateau in the amount of product generated is observed at earlier times in the binary mixtures and in ternary mixtures with low PSM content, and the extent of the reaction is higher in the raft mixtures with higher levels of PSM. Furthermore, the amount of PSM that remains in the ternary mixtures that define the raft region slightly decreases from T2 to T6, whereas for the other ternary and binary mixtures, the final PSM fraction is much higher (Fig. S1).

To better understand the relationship between the initial substrate concentration in the ternary mixtures and the amount of PCer generated, the data from Fig. 3 *A* were plotted as a function of X_{PSM} (Fig. 3 *B*). Of interest, up to 2 min of reaction time, X_{PCer} generation is similar in all the mixtures within the raft region. After 5 min, the profile of PCer generation changes and the amount of PCer formed is higher for the mixtures containing more PSM. Note that this is not valid for the ternary mixture containing higher PSM levels (T7) that lie outside the coexistence region in

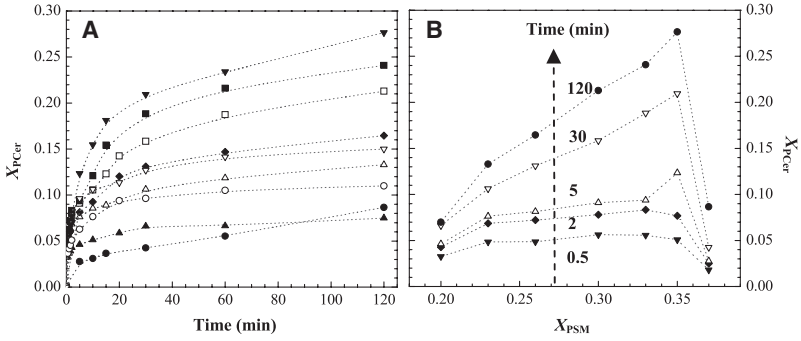

FIGURE 3 Amount of PCer generated by PSM hydrolysis by SMase. (*A*) Fraction of PCer formed versus time in (○) 30% and (▽) 40% PSM-containing binary mixtures and in POPC/PSM/Chol ternary mixtures containing (▲) 20 (T1), (△) 23 (T2), (◆) 26 (T3), (□) 30 (T4), (■) 33 (T5), (▼) 35 (T6), and (•) 37% (T7) PSM, respectively. (*B*) Relationship between the fraction of PCer formed and the initial substrate available for hydrolysis in POPC/PSM/Chol ternary mixture at (▼) $t = 0.5$, (◆) 2, (△) 5, (▽) 30, and (•) 120 min, respectively. The values are the means of at least three independent experiments. The SD was always <3%.

the POPC/PSM/Chol phase diagram. After 30 min, there is a linear correlation between the product formed and the amount of initial substrate, but again only for the mixtures in the raft region.

To test whether the rate of the enzymatic reaction was directly responsible for the observed rate of product formation, the initial rate of the reaction, V_0, was determined. V_0 corresponds to the first 2 min of reaction, before an alteration in the slope of the curve occurs, with a consequent decrease in the reaction rate. Fig. 4 shows the dependence of V_0 on membrane composition. As expected for the ternary mixtures that lie outside the l_d-l_o coexistence region, the initial reaction rate is lower than for those within the raft region. For these mixtures, V_0 initially increases until a certain PSM (or Chol; see below) concentration is reached, and decreases afterward. Of interest, the pattern of variation is not directly correlated to the total substrate in the mixtures, suggesting that other factors are governing the amount of PCer generated at the beginning of the reaction. Because the above data suggest a direct relationship between membrane properties and SMase activity, it is likely that the parameter dictating V_0 is the effective amount of PSM available for hydrolysis, and not the total amount of this lipid; that is, although more PSM is present in the mixtures with a higher l_o phase fraction, most of the substrate is involved in the formation of this phase with Chol. Due to the strong interactions between these lipids, and the high order of the phase formed, less PSM is accessible to the enzyme. Indeed, it was previously shown that SMase preferentially hydrolyzes substrate at the boundaries of l_o domains (17,19). As the reaction proceeds, the composition of the mixtures changes and the PSM/Chol-enriched l_o phase is lost, and thus a Chol-enriched/PSM-depleted l_o phase predominates. Under these conditions, more substrate is present in a more disordered phase. Furthermore, as shown in Fig. 3 *B*, as the time of reaction proceeds, the amount of X_{PCer} generated correlates linearly with PSM levels.

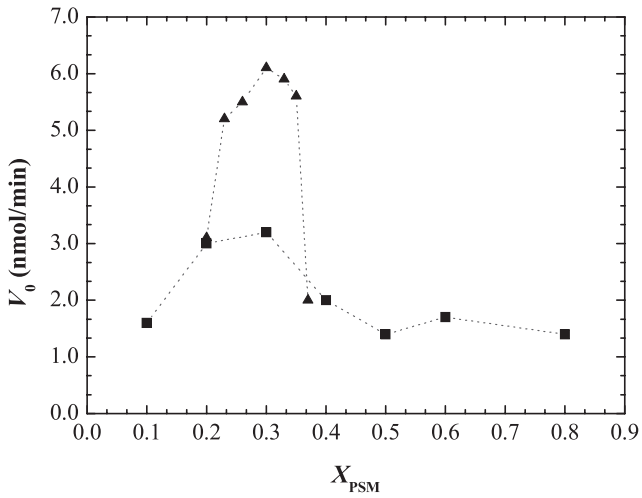

FIGURE 4 Dependence of the SMase initial reaction rate, V_o, on the amount of PSM. The initial rate of the reaction, V_o, was determined from the slope of a straight line tangent to the initial points of hydrolysis (2 min) in (■) binary POPC/PSM and ternary (▲) POPC/PSM/Chol mixtures, respectively.

Regarding the binary mixtures, V_0 slightly increases until 30% PSM is reached, and decreases afterward for higher PSM concentrations. This pattern is compatible with the binary phase diagram in which gel-fluid phase separation occurs at ~30% PSM (25). This suggests that the existence of a gel-fluid phase separation does not activate the enzyme, even though it introduces packing defects in the membrane. It should also be stressed that the reaction rates determined for SMase in the binary mixtures are lower than those obtained in the ternary ones, showing once again that even for higher substrate concentrations in the l_d phase (e.g., B30), enzyme activity is higher in raft mixtures.

Effect of SMase-generated PCer on membrane physical properties

To study the effect of PCer generation on membrane physical properties, the variation in t-PnA fluorescence anisotropy was measured during the time course of the SMase reaction in binary and ternary lipid vesicles with different lipid compositions and phase properties. This probe is very sensitive to the formation of Cer-gel domains because its fluorescence lifetime (and thus its quantum yield) strongly increases in the gel phase (28), and, in addition, it presents a high partition coefficient toward Cer-gel domains (8,9,15). Moreover, when these domains are formed, the fluorescence anisotropy of t-PnA also sharply increases as a consequence of their high order (15). From Fig. 5, it is possible to conclude that the effect of PCer is dependent on the initial membrane properties. In vesicles in the fluid (l_d) phase (both binary and ternary; Fig. 5 *A*), the addition of SMase leads to an instantaneous increase in t-PnA anisotropy, showing that 1), the enzyme action is very fast, as shown above and in agreement with previous studies (19,35,36); and 2), PSM hydrolysis instantly drives an alteration in membrane properties through the formation of a PCer-enriched gel phase. After ~5 min of reaction, t-PnA anisotropy reaches a plateau and remains invariant up to 2 h, although more PCer is formed during this time period (Fig. 3 *A*). As mentioned above, this is because the partition of t-PnA into the PCer-rich gel phase is very high and fast (9,15), and therefore readily reports the formation of this phase. In this way, the subsequent increase in the amount of PCer formed and, as a consequence the increase in PCer-rich gel phase, does not drive additional variation in the photophysical properties of the probe. Note that these anisotropy values indicate the coexistence of a PCer-enriched gel phase and a PCer-poor fluid phase, and therefore are lower compared to those obtained for a pure gel phase (15) (Fig. 5 *B*) (see below for gel phase fraction determination).

In vesicles in the l_o phase (T6; Fig. 5 *B*), t-PnA anisotropy is high and typical of this phase (9) but remains invariant

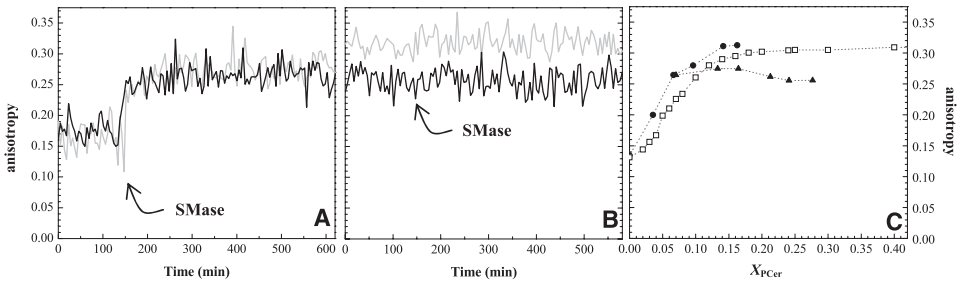

FIGURE 5 t-PnA fluorescence anisotropy in SMase-generated PCer mixtures. (*A* and *B*) Variation in the fluorescence anisotropy as a function of time in (*A*) l_d POPC/PSM 80:20 binary (*gray*) and POPC/PSM/Chol 72:23:5 ternary (T2) mixtures (*black*); and (*B*) (*black*) l_o POPC/PSM/Chol 25:35:40 ternary mixture (T6) and (*gray*) POPC/PSM 40:60 gel binary mixture. The arrow indicates the time at which SMase was added to the mixture. (*C*) t-PnA fluorescence anisotropy in (●) POPC/PSM and (▲) POPC/PSM/Chol 2 h after SMase addition. For comparison, t-PnA anisotropy in (□) POPC/PCer binary mixtures (15) is also plotted.

upon PCer generation, showing that under these conditions PCer-gel domain formation is minimal. This is further supported by t-PnA anisotropy in a gel-phase binary mixture (B60; Fig. 5 *B*) where the values are much higher than in the l_o phase. For this binary mixture, the formation of PCer also does not drive changes in t-PnA fluorescence anisotropy because a PSM gel phase is being converted into a PCer gel phase. Therefore, membrane order is not strongly affected by the reaction, leading to a constant and high anisotropy that is typical of a gel phase.

Fig. 5 *C* shows the variation in t-PnA anisotropy as a function of PCer generated after 2 h of reaction (as determined from Fig. 3 *A*) in binary and ternary mixtures. The data reveal the following: 1), For the binary mixtures, anisotropy increases with PCer and the values are much higher than in POPC/PCer binary mixtures (15) with the same PCer content, indicating that PCer and PSM associate to form gel domains, as previously shown in preformed mixtures containing PSM and PCer (8,9). 2), The amount of PCer generated in the ternary mixtures is higher than in the binary mixtures containing the same initial substrate concentration, showing once again that l_d-l_o phase coexistence facilitates enzyme activity. 3), In the ternary mixtures with lower PCer content, t-PnA anisotropy is high, showing that PCer is also able to recruit PSM to form gel domains. 4), With higher PCer content, the anisotropy decreases, in contrast to what is expected when more PCer is available to form a gel phase. This suggests that when more Chol is present in the mixtures, the ability of PCer to form gel domains diminishes. Plotting the data as a function of Chol content before and 2 h after SMase action (Fig. 6 *A*) shows that the anisotropy of t-PnA is higher for mixtures in the low-Chol range than for those in the high-Chol range. Note that in the absence of enzyme, t-PnA anisotropy increases with

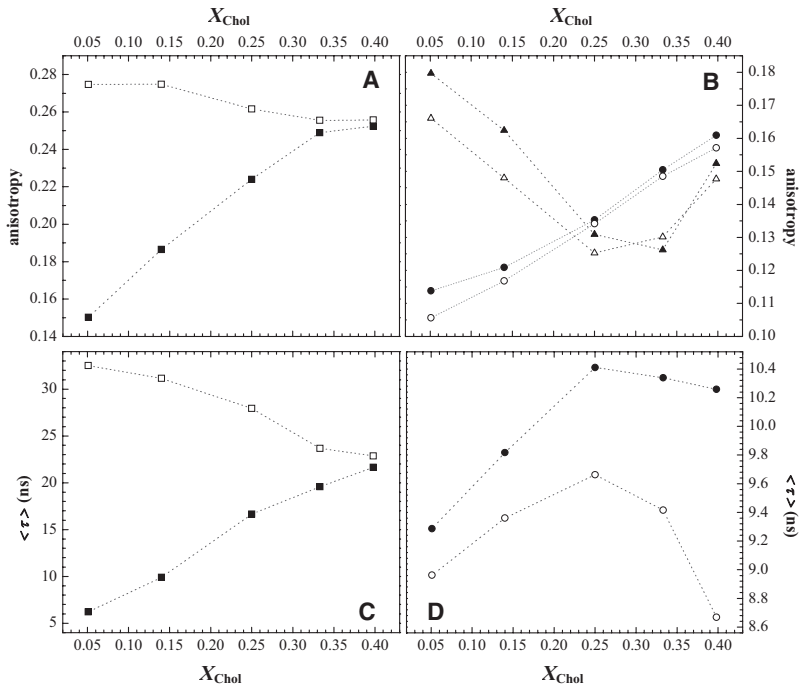

FIGURE 6 PCer-induced alterations in the membrane physical properties of raft mixtures. Fluorescence anisotropy of (*A*) (■,□) t-PnA, and (*B*) (▲,△) Rho-DOPE and (●,○) NBD-DPPE in the absence of SMase (*solid symbols*) and 2 h after SMase addition (*open symbols*). The mean fluorescence lifetimes of (*C*) t-PnA and (*D*) NBD-DPPE are shown (the symbols are the same as in *A* and *B*, respectively). The values are the means of at least three independent experiments. The SD was always lower than (*A* and *B*) 0.01, (*C*) 2 ns for t-PnA, and (*D*) 0.5 ns for NBD-DPPE.

Chol due to formation of the l_o phase, whereas it decreases in the presence of enzyme because the ability of PCer to segregate into gel domains diminishes. This is further supported by the anisotropy variation of Rho-DOPE (a typical l_d probe (9)) (Fig. 6 *B*) for the same mixtures. In the absence of SMase and with increasing Chol levels, fluorescence anisotropy decreases due to an increase in the l_o phase and a consequent decrease in the surface area available (i.e., the l_d phase) for probe distribution. Thus, due to energy homotransfer among Rho molecules, the anisotropy decreases (9,26). In the low-Chol range where PCer gel domains are formed, the probe is excluded and anisotropy decreases as a consequence of an even more efficient energy homotransfer. For higher Chol content, the anisotropy is similar in the absence and presence of SMase, demonstrating that PCer segregation into gel domains decreases.

Anisotropy data obtained with NBD-DPPE, a typical l_o probe (9) (Fig. 6 *B*), show the same pattern, i.e., PCer generation leads to a decrease in the anisotropy of the probe only in the low-Chol range because the probe is excluded from the gel phase and energy homotransfer increases.

Fig. 6 *C* shows that the profile of variation of t-PnA's mean fluorescence lifetime in the absence and 2 h after initiation of the enzyme reaction is similar to that obtained for anisotropy (Fig. 6 *A*), further supporting the above conclusions. Additionally, the high mean fluorescence lifetime values in the low-Chol range are a fingerprint of a PCer-rich gel phase (9). For NBD-DPPE, the mean fluorescence lifetime increases with Chol in both the absence and presence of SMase (Fig. 6 *D*). However, in the presence of the enzyme, the values are lower in all of the mixtures due to the occurrence of dynamic self-quenching. In the low-Chol range, PCer-gel domain formation leads to a decrease in the area available for probe distribution and a consequent increase in dynamic self-quenching. At higher Chol content, where the ability of PCer to segregate into the gel phase is lower, the increase in dynamic self-quenching can be explained by an increase in membrane fluidity, and therefore in diffusion of the probe, because the order of a PSM-depleted l_o phase is lower than that in a PSM-enriched phase (25).

With the use of t-PnA fluorescence lifetime and anisotropy data, and knowledge of both of the photophysical parameters of the probe in a PCer gel phase and its gel-fluid partition coefficient (15), the amount of gel phase (X_G) formed by PCer can be estimated (see Eqs. 2 and 4 in Silva et al. (9), and Eqs. S1 and S2). Fig. 7 shows the variation of X_G as a function of the PCer generated, the total sphingolipid present (PSM+PCer), or the Chol content in the mixtures. For comparison, X_G formed by PCer in POPC/PCer binary mixtures is also plotted. The data show that X_G formed by PCer in the low-Chol range is higher than that expected for the same amount of PCer in POPC, further supporting the ability of this lipid to recruit PSM. Moreover, for the lowest Chol content, almost all of the PCer and PSM are involved in PCer/PSM gel formation. In contrast, the increase in PCer leads to a decrease in X_G until

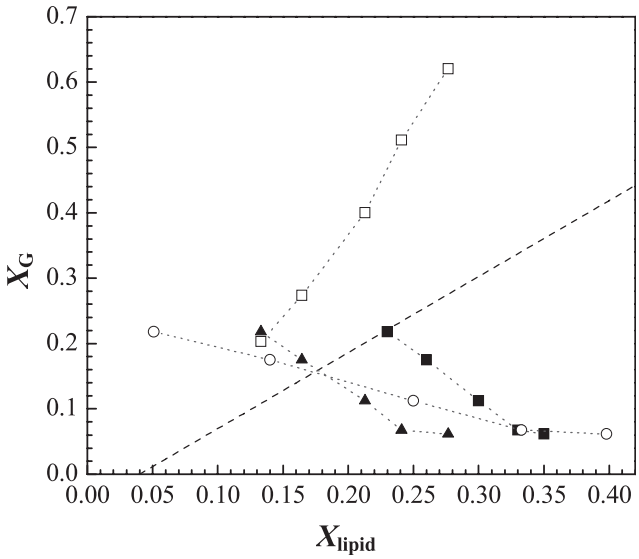

FIGURE 7 Amount of gel phase formed in the raft mixtures as a function of (▲) PCer generated, (■) total SL (PSM+PCer) present in the mixtures, and (○) Chol content. (□) X_G predicted from the ternary POPC/PSM/PCer phase diagram (Fig. 1 *B*) assuming that Chol is not affecting the interactions among the three other lipids. The dashed line corresponds to the amount of PCer-gel phase formed in POPC/PCer mixtures (15). See text and in the Supporting Material for further details on X_G determination.

only a small fraction is present, further showing the reduced ability of this lipid to segregate into a gel phase in a membrane enriched in Chol. Note that X_G linearly decreases with Chol content until 33 mol % Chol is reached.

Fig. 7 also shows the amount of gel phase that is directly determined from a POPC/PSM/PCer ternary phase diagram (Fig. 1 *B*) (8) assuming that the composition of the mixtures is given by the ratio between POPC, the amount of substrate remaining, and the product formed 2 h after the reaction begins. Under these conditions, if Chol were not affecting the interaction between these lipids, X_G would increase sharply with PCer. For the lowest Chol content, this assumption is valid, i.e., the amount of PCer/PSM gel formed is similar to that predicted by the ternary POPC/PSM/PCer phase diagram, showing that Chol is not interfering with PCer's ability to drive gel-fluid phase separation. For the other mixtures, the gel phase fraction decreases, in contrast to predictions made from the ternary diagram, further supporting a role for Chol in regulating membrane properties.

The hypothesis that, in the lowest Chol range, PCer and PSM interact to form a ~22% gel phase (Fig. 7) without being significantly affected by Chol is further validated through application of the model of Snyder and Freire (37), which allows one to predict the depolarization for Rho-DOPE molecules due to a decrease in the surface area available for probe distribution. To account for the observed decrease in Rho-DOPE anisotropy in the presence of SMase (Fig. 6 *B*), a reduction in area of ~10.4 Å^2 is expected. This is similar to the area occupied by POPC, PSM, and PCer involved in the formation of gel phase in the mixture (~10.2 Å^2), confirming the presence

of a gel fraction of ~22% (see text in the Supporting Material for details about the parameters used in the calculations).

In summary, the data presented above demonstrate that SMase readily drives the formation of PCer, and that the effects induced by this lipid are dependent on the initial and subsequent changes in membrane properties and composition.

Effect of SMase-generated PCer on lipid lateral organization

To further study how PCer generation affects lipid lateral organization, FRET studies were carried out between D/A pairs that preferentially partition into the different phases (9): t-PnA/NBD-DPPE (D/A 1) and NBD-DPPE/Rho-DOPE (D/A 2) D/A pairs report the changes in the gel/l_o phase and the l_o/l_d phase, respectively.

Fig. 8 *A* shows that 2 h after initiation of the enzyme reaction, FRET efficiency for the gel/l_o Förster pair (D/A 1), E, is lower in the low-Chol range due to PCer-gel phase formation. This is because t-PnA partitions preferentially into the gel phase, and NBD-DPPE partitions preferentially into the fluid phase. Under these conditions, the formation of a gel phase leads to an increase in the distance between donors and acceptors, and therefore to a decrease in E. Increasing Chol decreases PCer segregation into gel domains, which is translated by an increase in E. Note that for 33% Chol, the concentration at which the level of PCer gel is significantly decreased, E becomes similar in the absence and presence of SMase.

For the NBD-DPPE/Rho-DOPE (D/A 2) pair (Fig. 8 *B*) in the low-Chol range, E after enzyme reaction is higher due to PCer-gel domain formation. For this D/A pair, both probes are excluded from the PCer-gel phase, and therefore as the area for probe distribution decreases, the separation distance between D and A also decreases, leading to a higher E. It is possible to determine the expected increase in FRET efficiency assuming an ~10.2 Å^2 area reduction (see previous section) due to formation of the ~22% gel phase, and that both D and A randomly distribute in the l_d phase. Under these conditions, E should increase to ~65.7%, a value that is in agreement with the experimental one (~66.5%; see text in the Supporting Material for details on the model).

When the Chol content increases, there is only a slight decrease in E for the NBD-DPPE/Rho-DOPE (D/A 2) pair (Fig. 8 *B*) after PCer generation. Moreover, FRET efficiency is higher compared to that for the mixtures in the absence of enzyme. This could be attributed to PCer-gel phase formation as explained for the low-Chol range. However, this cannot be the only explanation, since 1), photophysical parameters of the probes show that the amount of PCer-gel phase formed in the high-Chol range is low (Figs. 5 and 6); 2), FRET efficiency for t-PnA/NBD-DPPE (D/A 1) also shows that PCer is not able to segregate into a large amount of gel phase when in mixtures with high-Chol content; and 3), dynamic self-quenching of NBD-DPPE suggests an increase in the fluidity of the ordered phase due to a decrease in the PSM available for l_o phase formation. This decrease in the order of the l_o phase would result in a different D/A probe distribution, bringing donors and acceptors close together and thus a subsequent increase in E, when compared to the same mixtures in the absence of SMase. In fact, the partition of Rho-DOPE into a PSM-depleted/Chol-enriched l_o phase is higher compared to a PSM/Chol-enriched l_o phase (38). Moreover, E between this D/A 2 pair further supports the presence of a small amount of PCer-rich gel in a PSM-depleted/Chol-enriched l_o membrane.

By taking advantage of the t-PnA/NBD-DPPE (D/A 1) FRET data, one can estimate the size of gel domains formed by PCer/PSM when Chol content is low, because for this D/A pair the acceptor is excluded from these domains. Therefore, applying a FRET model that takes into account the existence of an exclusion area where acceptors are not able to partition will provide information regarding the size of the domains. These models were previously described in detail (9,26). The considerations and parameters used for the calculations are the same as those used by Silva et al. (9), with minor modifications to account for the hydrolysis of PSM and consequent generation of PCer (see text in the Supporting Material for details). It can be concluded that for the ternary mixture with lowest Chol content (T2), the hydrolysis of PSM leads to the formation of an ~22% gel phase comprised of small PCer/PSM-enriched gel domains with an average size of ~8.5 nm.

From the above, it is possible to conclude that PCer generation drives the formation of small gel domains in mixtures with low Chol content, whereas in the high-Chol range it changes the properties of the l_o phase through its depletion in PSM.

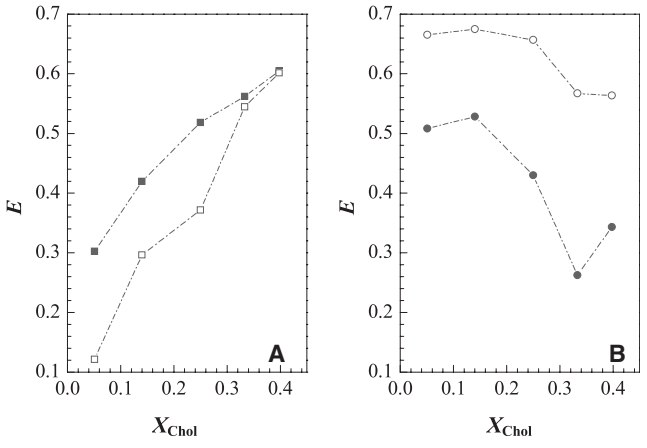

FIGURE 8 PCer-induced lateral lipid organization in raft mixtures. FRET efficiency, E, variation in the absence of SMase (*solid symbols*) and 2 h after SMase addition (*open symbols*) for (*A*) t-PnA/NBD-DPPE (D/A 1) and (*B*) NBD-DPPE/Rho-DOPE (D/A 2). The values are the average of at least three independent experiments, and the SD is <3%. Information regarding the relationship between gel/l_o and l_d/l_o phases is obtained from *A* and *B*, respectively. The fraction of gel phase present and the size of PCer/PSM-enriched gel domains formed in the lowest Chol content are determined from these FRET data. See text for further details.

DISCUSSION

Membrane properties and rafts control SMase activity

It is widely accepted that the interaction with the membrane of interfacial enzymes, such as phospholipase A2 (PLA2) and Chol oxidase, and the kinetic steps that lead to their adsorption to the interface, are highly regulated by the physical state of the membrane, in particular, the fluidity (23,34,40). Similar behavior has been described for SMase (12,20,22,41).

However, to fully understand how SMase activity is regulated, it is necessary to thoroughly explore the dependence of this enzyme on the membrane lipid composition and therefore on the membrane properties. This includes the initial physical state of the membrane, the lateral organization of the lipid phases, the concentration of substrate available for hydrolysis, and the partitioning of the substrate among the different phases. Such a detailed study becomes possible only after the phase diagrams of the relevant systems, i.e., POPC/PSM binary and POPC/PSM/Chol ternary mixtures (25), have been described. From the data in the current study, it is possible to conclude that SMase activity is strongly dependent on membrane properties and not on the amount of substrate. In binary mixtures, the extent and kinetics of hydrolysis decrease with PSM content and are very low in the ternary mixture with the highest PSM amount (Figs. 1 *B* and 2).

As previously suggested, SMase activity is regulated by the fluidity of the membrane (12,20), because it is higher in the fluid phase than in the gel phase. However, this relationship is not direct because otherwise the ability of SMase to hydrolyze PSM would increase in the sequence $l_d > l_d + l_o > l_d$ (fluid) + gel ~ l_o > gel. In contrast, it is evident that for a similar substrate concentration (e.g., 30% PSM) the amount of hydrolysis is higher within the l_d/l_o phase coexistence region (raft region) than in the l_d phase (Fig. 2). The existence of phase boundaries (domain interfaces) in the former mixtures could be a factor that governs the augmented SMase activity by facilitating its adsorption onto the membrane, as suggested for PLA2 (34). Moreover, using atomic force microscopy, Chiantia et al. (17) and Ira and Johnston (19) showed that SMase preferentially acts on the SM present at domain interfaces. However, the existence of domain interfaces is not likely to be the sole factor governing SMase activity, since in mixtures with gel-fluid phase coexistence, PSM hydrolysis decreases (Fig. 2). Previous studies carried out in gel phase (or liquid-condensed (LC)) membranes showed that gel-fluid (or LC-liquid expanded (LE)) phase separation increases SMase activity (20,43,44) due to boundary defects between the phases. Indeed, in comparison with a gel phase membrane (e.g., B80; Figs. 1 *B* and 2), the existence of gel-fluid phase boundaries strongly enhances SMase activity. However, in comparison with a single l_d phase, the extent of hydrolysis is lower (Fig. 2) and the reaction is slower (Fig. 4). Moreover, the initial reaction rate decreases in the binary mixtures when gel-fluid (l_d) phase separation is reached (>30% PSM). It was recently reported that in the presence of LC-LE SM/Cer monolayers, SMase is located in the LE phase and not at the boundaries (45), further showing that enzyme activity is not modulated only by packing defects.

It is therefore possible to conclude that SMase activity is higher in raft-like mixtures and strongly decreases in mixtures presenting a homogeneous fluid phase (i.e., only l_d or l_o), gel phase or gel-fluid phase coexistence, suggesting that in biological membranes lipid rafts have a key role in the regulation of SMase activity. These conclusions support the previous suggestion that lipid rafts are required for the activation of SMase (4).

Also of interest is the increased hydrolysis in the ternary mixtures compared to binary mixtures containing identical phase properties and substrate concentration. For instance, 5% Chol in mixture T2 leads to 20% more hydrolysis as compared to mixture B20, which are both in the l_d phase. It was previously shown that Chol leads to an increase in SMase activity (11,20). However, this was suggested to be due to an increase in fluidity compared to the other mixtures under study, which were typically in the gel phase. In the study presented here, both mixtures were in the l_d phase, and the fluidity was similar. Therefore, in this case, it is likely that the role of Chol depends on its ability to segregate PSM with a consequent increase in the local concentration of the substrate available for hydrolysis. In addition, the difference in size of the two lipids may facilitate the adsorption of the enzyme to the interface.

However, this is not valid when the Chol content is high, and thus when the l_o phase is predominant. Despite the higher local PSM concentration, the initial interaction of SMase appears to decrease, as shown by the variation in the initial rate of hydrolysis, which slightly decreases for raft mixtures containing a high l_o fraction (T5 and T6), and is very low when only the l_o phase is present (T7) (Fig. 4). For these lipid compositions, SMase has to interact with PSM molecules that are involved in the formation of the l_o phase and thus are more ordered. As a consequence, although PSM content is higher in these mixtures, the amount of PCer initially generated (2 min) is similar in all of the mixtures. As the reaction proceeds, the l_o phase is perturbed and the amount of PCer generated now becomes dependent on the amount of available PSM. Under these conditions, the order of the l_o phase decreases (as also suggested by data obtained with NBD-DPPE; Figs. 6 and 8) because it becomes PSM-depleted, augmenting the diffusion of both enzyme and substrate. It is also likely that the initial formation of PCer facilitates SMase catalysis by increasing the local enzyme concentration at the boundary interfaces, as previously reported for SMase in other ternary mixtures containing Chol and SM (17,19). For these mixtures X_G PCer is very low. Moreover, if the enzyme preferentially acts at the boundaries between these fluid phases, when the

l_o fraction becomes very high (from T1 to T7), the number of boundaries will decrease as a consequence of the larger size of the rafts (26), further explaining the decrease in the initial rate of catalysis. In agreement with the variation in the initial rate of reaction (Fig. 4) is the fact that large raft domains are observed for mixtures containing $X_{Chol} \geq 33\%$ (26).

Another important point that should be taken into consideration is the ability of SMase to hydrolyze more than 50% of SM only in the ternary raft mixtures, which shows that, for these mixtures, SM in the inner leaflet becomes available to the enzyme. From our data it is not possible to establish the mechanism by which SM becomes exposed to the enzyme. Previous studies suggested that this may be due to an increased ability of SM to translocate across the membrane as a consequence of Cer formation, or to perturbations in the structure of the membrane (11,36). Such alterations in the membrane make it difficult to perform kinetic analyses of SMase activity for longer time periods, and therefore we made no attempt to further interpret the SMase activity.

PCer-induced physical changes are dependent on membrane lipid composition

It is widely accepted that Cer generation leads to strong alterations in the membrane biophysical properties and lipid organization in both model and cell membranes (6). However, it should be stressed that the effects of Cer are largely dependent on membrane composition, e.g., in the presence of phosphoethanolamine-containing lipids, Cer facilitates the formation of nonlamellar phases (14), which has not been observed for PC-containing lipids (7,15,17). Therefore, to know how Cer generation affects the membrane, it is necessary to determine the relationship between the lipid composition and Cer-induced alterations.

SMase activity is dependent on the membrane composition and properties; consequently, the amount of PCer generated, and thus the PCer-induced changes, also depend on these factors. In a gel phase mixture (e.g., B80), the amount of PCer formed is minimal and, in addition, the conversion of a PSM-gel into a PCer-gel phase does not lead to strong alterations in the physical properties of the membrane (Fig. 5 *B*). For this particular mixture, the hydrolysis of PSM leads to the formation of a PCer-rich gel phase that segregates from the PSM-rich gel phase (Fig. 1 *B*). The amount of PCer-gel formed is obtained from the ternary POPC/PSM/PCer phase diagram (Table 1), further showing that although a relatively high fraction is formed, the physical properties remain unchanged.

In the l_o phase (sample T7), a very low amount of PCer is generated, but also no significant changes are detected upon PSM hydrolysis (Fig. 5 *B*). In this case, the high Chol content inhibits PCer-gel phase formation and the membrane remains in the l_o phase.

In contrast, the generation of PCer in the l_d phase greatly alters the membrane physical properties through the formation of PCer/PSM-enriched gel domains (Fig. 5 *A*). The amount of this new phase depends on the initial contents of both PSM and Chol (see Table 1). It should be stressed that, in this case, a low amount of Chol (compare samples T2 and B20) favors gel-phase formation because a higher amount of PSM is hydrolyzed (Figs. 2 and 3, and Table 1).

TABLE 1 Lipid composition (X_{lipid}) and fraction of gel phase (X_G)* formed in the mixtures 2 h after initiation of the SMase reaction

	POPC/PSM	X_{POPC}	X_{PSM}	X_{Chol}	X_{PCer}	X_G[†]	$X_{G(PCer)}$[‡]
B10	90:10	0.90	0.04	–	0.06	0.04	–
B20	80:20	0.80	0.12	–	0.08	0.12	–
B30	70:30	0.70	0.18	–	0.12	0.22	–
B40	60:40	0.60	0.26	–	0.14	0.42	–
B50	50:50	0.50	0.36	–	0.14	0.56[§]	0.50[§]
B60	40:60	0.40	0.44	–	0.16	0.77[§]	0.60[§]
B80	20:80	0.20	0.67	–	0.13	1.00[¶]	0.33[¶]
	POPC/PSM/Chol						
T1	80:20:0	0.80	0.12	–	0.08	0.12	–
T2	72:23:5	0.72	0.10	0.05	0.13	0.22	–
T3	60:26:14	0.60	0.10	0.14	0.16	0.17	–
T4	45:30:25	0.45	0.09	0.25	0.21	0.11	–
T5	34:33:33	0.34	0.09	0.33	0.24	0.07	–
T6	25:35:40	0.25	0.07	0.40	0.28	0.06	–
T7	15:37:48	0.15	0.28	0.48	0.09	–	–

*X_G was determined from the POPC/PSM/PCer phase diagram and from the photophysical parameters of t-PnA for the binary and ternary mixtures, respectively. See text and in the Supporting Material for details.

[†,‡]For a situation in which two gel phases coexist, X_G is the total gel phase present in the mixtures and $X_{G(PCer)}$ is the fraction of PCer-enriched gel phase.

[§]These mixtures lie within the three-phase region of the diagram and therefore contain PCer-gel and PSM-gel phase separation.

[¶]These mixtures lie within the two-gel-phase coexistence region.

PCer-induced alterations in raft mixtures are more complex and extremely dependent on Chol content. PCer segregates together with PSM to form small (~8.5 nm) PCer/PSM-enriched gel domains when the Chol content is low, and at higher Chol concentrations the amount of gel phase formed decreases and becomes PCer-enriched/PSM-depleted (Figs. 6–8). From these results it is possible to conclude that Chol strongly influences the ability of PCer to segregate into gel domains. In addition, the ratio between PCer-formed and Chol present (X_{PCer}/X_{Chol}) (Fig. S2) further shows that 1), PCer/PSM-enriched gel phase is formed when PCer content is higher than Chol (i.e., $X_{PCer}/X_{Chol} > 1$); 2), the gel phase is depleted in PSM and enriched in PCer when the ratio approaches one; and 3), when $X_{PCer}/X_{Chol} < 1$, the PCer-gel phase strongly decreases and the Chol-enriched l_o phase dominates. Therefore, our results strongly support the hypothesis that the amount of Chol in the membrane constitutes a mechanism to regulate the effects of Cer. In this context, it is expected that the probability of Cer-enriched domain formation and, consequently, the activation of a specific Cer-dependent process is higher in a membrane poor in Chol. On the other hand, from a physical standpoint,

a membrane rich in Chol is less susceptible to Cer formation, and therefore the activation of processes that depend on alterations in the membrane biophysical properties are less likely. Of interest, PCer-induced physical alterations in the studied raft mixtures are strongly reduced when the initial POPC/PSM/Chol lipid composition is 1:1:1, the canonical raft mixture that is commonly ascribed as the typical cell membrane raft composition (32).

SMase activity is dependent on PCer-induced membrane physical alterations

SMase is regulated by the initial lipid composition; however, it is also dependent on the product formed (22). A closer examination of the relationship between the final lipid composition and the amount of gel phase formed (Table 1) shows that SMase is inhibited when this phase is present. This is clearly seen in raft mixtures, where the amount of substrate remaining after hydrolysis decreases with Chol content. In these mixtures, the extent of hydrolysis is higher due to the ability of Chol to prevent PCer-gel phase formation to a great extent, i.e., SMase activity is not inhibited because the gel phase is kept to a minimum and the substrate remains available in a more fluid phase. Furthermore, it is clear from the variation of the amount of PCer formed (Fig. 3 *A*) that a plateau in product formation is attained at longer times when the Chol content is higher. Our results on the extent of hydrolysis (Fig. 2) and rate of reaction (Fig. 4) are similar to those reported by Fanani and Maggio (23), who also observed inhibition of the enzyme by the product of reaction, further supporting a role of PCer in the modulation of SMase activity.

Another important factor should be taken into account concerning the mechanism of SMase regulation, and this is related to the ability of PCer to recruit PSM (8,9). The interaction between these lipids leads to a local increase in substrate concentration, which facilitates the reaction by bringing the substrate closer to the enzyme. As the reaction proceeds, two situations are possible, depending on the membrane composition (Fig. 9): 1), the gel phase fraction is low and thus PSM hydrolysis continues (high Chol; Fig. 9 *B*) until only a small fraction of PSM remains in the membrane; or 2), the local increase in PCer drives PCer/PSM-enriched gel domains (low-Chol; Fig. 9 *A*) that on the one hand negatively regulate SMase, and on the other can trap molecules involved in signaling cascades.

In the binary mixtures, independently of their composition, PCer drives the formation of the gel phase (either a PCer/PSM-gel or a PCer- and PSM-gel; see Table 1 for further information regarding the gel phase fraction) and therefore the extent of the reaction is lower. In comparison to the ternary mixtures, a plateau in the amount of PCer formed is reached at a lower quantity, further showing that PSM hydrolysis is stopped at earlier times (Fig. 3 *A*). Note that for the situation that mimics gel-fluid phase separation, i.e., LE-LC phase separation in monolayers, SMase locates and exerts its action preferentially in an LE phase, whereas the Cer-LC phase strongly decreases the catalytic rate of the enzyme (45). In addition, enzyme activity is virtually abolished as the gel phase increases, as also shown for SM/Cer monolayers when LC percolation was attained (43).

CONCLUSIONS

The study described herein allowed analyses of the interplay among the SMase activity, membrane composition and properties, quantity of PCer-generated, and PCer-induced biophysical alterations. In this regard, it is possible to conclude that SMase activity strongly depends on the initial membrane properties and is regulated by the alterations induced by PCer. On the other hand, PCer-induced changes are also dependent on membrane properties, not only because of the extent of product generated, but also because of the initial lipid composition. Playing a key role in this interplay is Chol, which may function as a regulatory molecule in this process. Chol is required for the formation of lipid rafts in both model (25) and cell (48) membranes, and lipid rafts were shown here to regulate both enzyme activity and Cer-induced effects. It is therefore likely that Chol in particular, and lipid rafts in general, function as modulators of SMase in the cells. In fact it has been reported that lipid rafts are required for the activation of SMase in cells (4), further corroborating the hypothesis that rafts have a dual role in the regulation of enzyme-Cer interplay.

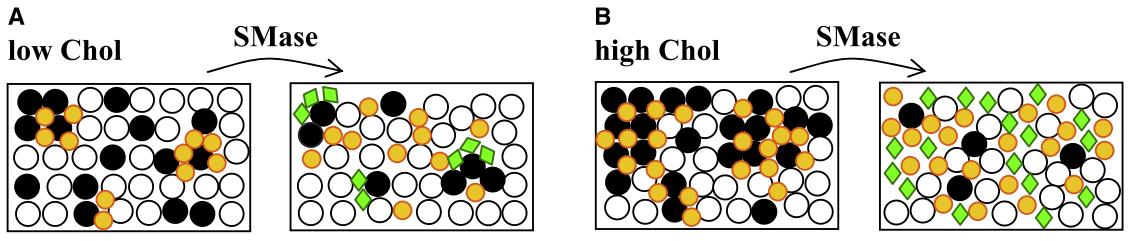

FIGURE 9 Schematic representation of SMase effects on raft membranes. (*A*) In the low-Chol range (small raft-size range, *left panel*), small PCer/PSM-enriched gel domains are formed upon PSM hydrolysis (*right panel*). (*B*) When Chol content is high (large raft-size range, *left panel*), SMase-generated PCer is not able to induce gel domain formation and l_o-phase Chol-enriched/PSM-depleted predominates (*right panel*). The symbols represent (*open circle*) POPC, (*solid circle*) PSM, (*small circle*) Chol, and (*diamond*) Cer.

Also important is the ability of SMase to instantaneously drive Cer formation, placing Cer once more as a key lipid in the modulation of biological processes. However, it is important to define the properties and the concept of the so-called ''platforms'', because if they are Cer-enriched they should segregate in the membrane as gel phase domains that are formed under specific lipid composition conditions. Moreover, it is implicit that ''platforms'' are large domains and Cer-domains are small (Fig. 9 *A*). On the other hand, if the term ''platforms'' refers only to the large domains that form upon Cer generation in Chol-enriched membranes, such domains have distinctly different properties compared with the Cer-enriched domains and are likely to be Chol-enriched/PSM-depleted l_o domains (Fig. 9 *B*).

The physical properties of the domains formed, therefore, will differ depending on the amount of Chol present in the membrane. In this context it is essential to establish whether Cer generation is involved in the regulation of biological processes, and whether the different alterations in the membrane induced by Cer constitute a mechanism to regulate a specific process. It is not unlikely that the formation of very rigid and compact Cer-enriched domains results in membrane areas that would present a higher tendency to exclude signaling molecules, which would be better accommodated in the less-ordered Chol-enriched domains. Therefore, the ability of Chol to regulate the outcome of Cer can be a means to determine which process will be activated.

Although biological membranes are much more complex than the model membranes used in this study, especially when considering protein and lipid composition, inner and outer leaflet asymmetry, and processes that modify membrane lipid composition (e.g., lipid hydrolysis/synthesis, lipid flip-flop), it is likely that the general principles presented here do indeed describe the interplay among raft lipid composition, SMase activity, and Cer-induced alterations in biomembranes. For instance, studies carried out in asymmetric planar membranes show that strong interleaflet interactions occur and domain formation takes place even in the absence of proteins and despite the ability of one of the leaflets to form domains, in a manner similar to that observed in symmetric model membranes (49). Moreover, it was shown here that SMase activity and Cer-induced changes are mainly dependent on the raft lipid composition, especially the Chol content, and therefore on the raft physical properties. Because of the high enrichment of Chol and SM in the outer leaflet of the plasma membrane, raft domains form mainly on this membrane side (1). Therefore, the lipid vesicles used mimic the outer leaflet of the plasma membrane. From the biological perspective, an important observation results from the ability of Cer to promote transbilayer movement in raft mixtures, corroborating the previous hypothesis that activation of internal signaling cascades may indeed be modulated by Cer generated in the outer leaflet (11,41,50), either by direct activation of proteins (51) or as a result of interleaflet domain coupling (52) or even lipid interdigitation (53).

SUPPORTING MATERIAL

Ten equations and two figures are available at http://www.biophysj.org/biophysj/supplemental/S0006-3495(09)00391-9.

We thank Alexander Fedorov for assistance in the time-resolved fluorescence measurements, and Rodrigo F. M. de Almeida for helpful discussions. A. H. Futerman is the Joseph Meyerhoff Professor of Biochemistry at the Weizmann Institute of Science.

This work was supported by the Fundação para a Ciência e Tecnologia (grant BPD/30289/2006 to L.C.S., and grants POCTI/QUI/57123/2004 and POCTI/QUI/68151/2006) and the Israel Science Foundation (1735/07).

REFERENCES

1. Rajendran, L., and K. Simons. 2005. Lipid rafts and membrane dynamics. *J. Cell Sci.* 118:1099–1102.
2. Futerman, A. H., and Y. A. Hannun. 2004. The complex life of simple sphingolipids. *EMBO Rep.* 5:777–782.
3. Holthuis, J. C. M., G. van Meer, and K. Huitema. 2003. Lipid microdomains, lipid translocation and the organization of intracellular membrane transport. *Mol. Membr. Biol.* 20:231–241, [Review].
4. Bollinger, C. R., V. Teichgraber, and E. Gulbins. 2005. Ceramide-enriched membrane domains. *Biochim. Biophys. Acta.* 1746:284–294.
5. Gulbins, E., S. Dreschers, B. Wilker, and H. Grassme. 2004. Ceramide, membrane rafts and infections. *J. Mol. Med.* 82:357–363.
6. Kolesnick, R. N., F. M. Goni, and A. Alonso. 2000. Compartmentalization of ceramide signaling: physical foundations and biological effects. *J. Cell. Physiol.* 184:285–300.
7. Hsueh, Y. W., R. Giles, N. Kitson, and J. Thewalt. 2002. The effect of ceramide on phosphatidylcholine membranes: a deuterium NMR study. *Biophys. J.* 82:3089–3095.
8. Castro, B. M., R. F. M. De Almeida, L. C. Silva, A. Fedorov, and M. Prieto. 2007. Formation of ceramide/sphingomyelin gel domains in the presence of an unsaturated phospholipid: a quantitative multiprobe approach. *Biophys. J.* 93:1639–1650.
9. Silva, L. C., R. F. M. de Almeida, B. M. Castro, A. Fedorov, and M. Prieto. 2007. Ceramide-domain formation and collapse in lipid rafts: membrane reorganization by an apoptotic lipid. *Biophys. J.* 92:502–516.
10. Sot, J., F. M. Goñi, and A. Alonso. 2005. Molecular associations and surface-active properties of short- and long-N-acyl chain ceramides. *Biochim. Biophys. Acta.* 1711:12–19.
11. Contreras, F. X., A. V. Villar, A. Alonso, R. N. Kolesnick, and F. M. Goñi. 2003. Sphingomyelinase activity causes transbilayer lipid translocation in model and cell membranes. *J. Biol. Chem.* 278:37169–37174.
12. Ruiz-Argüello, M. B., M. P. Veiga, J. L. R. Arrondo, F. M. Goñi, and A. Alonso. 2002. Sphingomyelinase cleavage of sphingomyelin in pure and mixed lipid membranes. Influence of the physical state of the sphingolipid. *Chem. Phys. Lipids.* 114:11–20.
13. Goñi, F. M., and A. Alonso. 2007. Biophysics of sphingolipids I. Membrane properties of sphingosine, ceramides and other simple sphingolipids. *Biochim. Biophys. Acta.* 1768:1309–1310.
14. Sot, J., F. J. Aranda, M. I. Collado, F. M. Goñi, and A. Alonso. 2005. Different effects of long- and short-chain ceramides on the gel-fluid and lamellar-hexagonal transitions of phospholipids: a calorimetric, NMR, and x-ray diffraction study. *Biophys. J.* 88:3368–3380.
15. Silva, L., R. F. M. de Almeida, A. Fedorov, A. P. A. Matos, and M. Prieto. 2006. Ceramide-platform formation and -induced biophysical changes in a fluid phospholipid membrane. *Mol. Membr. Biol.* 23:137–150.
16. Holopainen, J. M., M. Subramanian, and P. K. J. Kinnunen. 1998. Sphingomyelinase induces lipid microdomain formation in a fluid phosphatidylcholine/sphingomyelin membrane. *Biochemistry.* 37:17562–17570.
17. Chiantia, S., N. Kahya, J. Ries, and P. Schwille. 2006. Effects of ceramide on liquid-ordered domains investigated by simultaneous AFM and FCS. *Biophys. J.* 90:4500–4508.

18. Ira and L. J. Johnston. 2006. Ceramide promotes restructuring of model raft membranes. *Langmuir*. 22:11284–11289.

19. Ira and L. J. Johnston. 2008. Sphingomyelinase generation of ceramide promotes clustering of nanoscale domains in supported bilayer membranes. *Biochim. Biophys. Act.* 1778:185–197.

20. Jungner, M., H. Ohvo, and J. P. Slotte. 1997. Interfacial regulation of bacterial sphingomyelinase activity. *Biochim. Biophys. Acta*. 1344:230–240.

21. Contreras, F. X., J. Sot, M. B. Ruiz-Argüello, A. Alonso, and F. M. Goñi. 2004. Cholesterol modulation of sphingomyelinase activity at physiological temperatures. *Chem. Phys. Lipids*. 130:127–134.

22. De Tullio, L., B. Maggio, S. Hartel, J. Jara, and M. L. Fanani. 2007. The initial surface composition and topography modulate sphingomyelinase-driven sphingomyelin to ceramide conversion in lipid monolayers. *Cell Biochem. Biophys.* 47:169–177.

23. Fanani, M. L., and B. Maggio. 1998. Surface pressure-dependent cross-modulation of sphingomyelinase and phospholipase A(2) in monolayers. *Lipids*. 33:1079–1087.

24. Fanani, M. L., and B. Maggio. 2000. Kinetic steps for the hydrolysis of sphingomyelin by *Bacillus cereus* sphingomyelinase in lipid monolayers. *J. Lipid Res*. 41:1832–1840.

25. De Almeida, R. F. M., A. Fedorov, and M. Prieto. 2003. Sphingomyelin/phosphatidylcholine/cholesterol phase diagram: boundaries and composition of lipid rafts. *Biophys. J.* 85:2406–2416.

26. De Almeida, R. F. M., L. M. S. Loura, A. Fedorov, and M. Prieto. 2005. Lipid rafts have different sizes depending on membrane composition: a time-resolved fluorescence resonance energy transfer study. *J. Mol. Biol.* 346:1109–1120.

27. Vierl, U., L. Lobbecke, N. Nagel, and G. Cevc. 1994. Solute effects on the colloidal and phase-behavior of lipid bilayer-membranes—ethanol-dipalmitoylphosphatidylcholine mixtures. *Biophys. J.* 67:1067–1079.

28. Sklar, L. A., B. S. Hudson, M. Petersen, and J. Diamond. 1977. Conjugated polyene fatty-acids on fluorescent-probes—spectroscopic characterization. *Biochemistry*. 16:813–819.

29. Haugland, R. 1996. Handbook of Fluorescent Probes and Research Chemicals Molecular Probes, Eugene, OR.

30. De Almeida, R. F. M., L. M. S. Loura, A. Fedorov, and M. Prieto. 2002. Nonequilibrium phenomena in the phase separation of a two-component lipid bilayer. *Biophys. J.* 82:823–834.

31. Loura, L. M. S., A. Fedorov, and M. Prieto. 2001. Fluid-fluid membrane microheterogeneity: a fluorescence resonance energy transfer study. *Biophys. J.* 80:776–788.

32. Veatch, S. L., and S. L. Keller. 2003. A closer look at the canonical 'raft mixture' in model membrane studies. *Biophys. J.* 84:725–726.

33. Rhines, F. N. 1956. Phase Diagrams in Metallurgy: Their Development and Application McGraw-Hill, New York.

34. Simonsen, A. C. 2008. Activation of phospholipase A2 by ternary model membranes. *Biophys. J.* 94:3966–3975.

35. Holopainen, J. M., M. I. Angelova, and P. K. J. Kinnunen. 2000. Vectorial budding of vesicles by asymmetrical enzymatic formation of ceramide in giant liposomes. *Biophys. J.* 78:830–838.

36. Ruiz-Argüello, M. B., G. Basáñez, F. M. Goñi, and A. Alonso. 1996. Different effects of enzyme-generated ceramides and diacylglycerols in phospholipid membrane fusion and leakage. *J. Biol. Chem.* 271:26616–26621.

37. Snyder, B., and E. Freire. 1982. Fluorescence energy-transfer in 2 dimensions—a numeric solution for random and nonrandom distributions. *Biophys. J.* 40:137–148.

38. De Almeida, R. F. M., J. Borst, A. Fedorov, M. Prieto, and A. J. W. G. Visser. 2007. Complexity of lipid domains and rafts in giant unilamellar vesicles revealed by combining imaging and microscopic and macroscopic time-resolved fluorescence. *Biophys. J.* 93:539–553.

39. Reference deleted in proof.

40. Slotte, J. P. 1995. Direct observation of the action of cholesterol oxidase in monolayers. *Biochim. Biophys. Acta.* 1259:180–186.

41. Contreras, F. X., G. Basanez, A. Alonso, A. Herrmann, and F. M. Goñi. 2005. Asymmetric addition of ceramides but not dihydroceramides promotes transbilayer (flip-flop) lipid motion in membranes. *Biophys. J.* 88:348–359.

42. Reference deleted in proof.

43. Fanani, M. L., S. Hartel, R. G. Oliveira, and B. Maggio. 2002. Bidirectional control of sphingomyelinase activity and surface topography in lipid monolayers. *Biophys. J.* 83:3416–3424.

44. Hartel, S., M. L. Fanani, and B. Maggio. 2005. Shape transitions and lattice structuring of ceramide-enriched domains generated by sphingomyelinase in lipid monolayers. *Biophys. J.* 88:287–304.

45. De Tullio, L., B. Maggio, and M. L. Fanani. 2008. Sphingomyelinase acts by an area-activated mechanism on the liquid-expanded phase of sphingomyelin monolayers. *J. Lipid Res.* 49:2347–2355.

46. Reference deleted in proof.

47. Reference deleted in proof.

48. Simons, K., and D. Toomre. 2000. Lipid rafts and signal transduction. *Nat. Rev. Mol. Cell Biol.* 1:31–39.

49. Collins, M. D., and S. L. Keller. 2008. Tuning lipid mixtures to induce or suppress domain formation across leaflets of unsupported asymmetric bilayers. *Proc. Natl. Acad. Sci. USA.* 105:124–128.

50. Grassme, H., J. Riethmuller, and E. Gulbins. 2007. Biological aspects of ceramide-enriched membrane domains. *Prog. Lipid Res.* 46:161–170.

51. Bourbon, N. A., J. Yun, and M. Kester. 2000. Ceramide directly activates protein kinase Cζ to regulate a stress-activated protein kinase signaling complex. *J. Biol. Chem.* 275:35617–35623.

52. Putzel, G. G., and M. Schick. 2008. Phase behavior of a model bilayer membrane with coupled leaves. *Biophys. J.* 94:869–877.

53. Pinto, S. N., L. C. Silva, R. F. M. de Almeida, and M. J. Prieto. 2008. Membrane domain formation, interdigitation and morphological alterations induced by the very long chain asymmetric C24:1 ceramide. *Biophys. J.* 95:2867–2879.